

# Effect of particle size on high-pressure methane adsorption of coal

Jie Zou and Reza Rezaee\*

Department of Petroleum Engineering, Curtin University, Western Australia, Australia

Received May 15, 2016; Accepted August 6, 2016

**Abstract:** Adsorbed gas cannot be neglected in the evaluation of coalbed methane and shale gas since a significant proportion of gas is stored in the form of adsorbed gas. Adsorbed methane of coal and shale has been widely studied by high-pressure methane adsorption experiment. In sample treatment of the experiment, the sample is crushed and sieved to a particular particle size range. However, how particle size influence high-pressure methane adsorption is still unclear. In this study, low-pressure nitrogen (N<sub>2</sub>) and high-pressure methane adsorption have been measured on coal samples with different particle size. According to N<sub>2</sub> sorption analysis, pore volume and surface area increase with particle size reduction. Pore size distribution of small pores (<10nm) changes among varying particle size. Pore volume proportion of small pores (<10nm) increases and pore volume proportion of big pores (>10nm) decreases with decreasing particle size. Decreasing particle size by crushing sample introduces new connectivity for closed pores to the particle surface. The responses of isotherms of high-pressure methane adsorption are different with different particle size. Methane adsorption at initial pressure (145psi) increases with decreasing particle size. Adsorption increase rate at high pressure (435-870psi) decreases with particle size reduction. This can be explained that fine sample has more pore volume and higher pore volume proportion of small pores (<10nm). Sample with particle size of 150-250µm has the highest Langmuir volume.

**Key words:** particle size, high-pressure methane adsorption, coal, shale gas

## 1 Introduction

Natural gas production in shale gas and coalbed methane is perspective, especially when taking gas adsorption properties into consideration. Hydrocarbon gas (mostly methane) can be stored in pores and fractures, and as adsorbed gas on organic and inorganic matter. However, heterogeneous pore structure and complex chemical composition in shale and coal make the quantification of gas storage challenging (Labani et al., 2013). To evaluate methane adsorption capacity under reservoir condition, one reliable and popular research method is high-pressure methane adsorption experiment (Chalmers and Bustin, 2007a; Chalmers and Bustin, 2007b; Ross and Bustin, 2009; Zhang et al., 2012; Gasparik et al., 2014).

Prior to the high-pressure adsorption experiment, the sample is crushed and sieved to a particular particle size. Surprisingly, different particle size has been used in high-pressure methane adsorption related studies (Ross and Bustin, 2009; Zhang et al., 2012; Gasparik et al., 2014). Table 1 shows particle size used in high-pressure methane adsorption related studies. A study by Clarkson and Bustin (1999) has suggested that a particle size of 4mesh (<4.75mm) and 60mesh (<0.250mm) coal sample has a negligible effect on high-pressure methane adsorption (Clarkson and Bustin, 1999). Another study on pure clay samples has shown that methane adsorption capacity of clay minerals increases with decreasing particle size because of the enlarged internal surface area (Ji et al., 2012). Furthermore, the effect of particle size on gas adsorption porosimetry and high-pressure

\* Corresponding author. Email: R.Rezaee@curtin.edu.au

CO<sub>2</sub> adsorption has been investigated as well (Chen et al., 2015; Lutynski and González González, 2016). The gas adsorption porosimetry study on shale has shown that micropore volume generally increases with particle size reduction. The high-pressure CO<sub>2</sub> adsorption study on coal and shale has shown that coal samples have different composition among varying particle size, and shale samples get extended surface area with decreasing particle size. Although high-pressure methane adsorption has been widely used, the effect of particle size on the high-pressure methane adsorption is not clear.

In this study, we measured high-pressure methane adsorption on the same coal samples but with different particle size. Low-pressure N<sub>2</sub> sorption was also engaged to give an insight into the pore structure of the studied samples. This study attempted to find out if and how particle size of sample influence high-pressure methane adsorption.

Table 1 Particle sizes used in high-pressure methane

Literature	Particle size (µm)
Gasparik et al, 2013	500-1000, <100
Ross and Bustin, 2009	<250
Chalmers and Bustin, 2012	<250
Zhang et al., 2012	150-500

## 2 Materials and methods

### 2.1 Materials

For the purpose of this study, the particle size of the sample was the only experimental variable. Herein, commercial coal provided by BM Alliance coal operations Pty Ltd was used. Table 2 shows the sample information. The mean vitrinite reflectance of the sample is 1.43%.

For the purpose of this study the original coal was sieved to four particle size range: <325mesh, 200-325mesh, 60-100mesh, and 18-20mesh.

Table 2 Composition of the studied sample

Telovitrinite (%)	71.1
Detrovitrinite (%)	3.7
Fusinite (%)	3.3
Semi-Fusinite (%)	13
Macrinite (%)	0.3
Inertodetrinite (%)	4
Mineral matter (%)	4.5

### 2.2 Methods

#### 2.2.1 High-pressure methane adsorption

High-pressure (up to 870psi) methane adsorption was measured

at 30°C by a commercial volumetric apparatus (High pressure volumetric analyzer) (Fig 1). The experiment setup basically consists of a vacuum pump, an outgassing furnace with a temperature controller, a sample cell, a thermostat bath connected with sample cell for controlling the experimental temperature and a reference cell connected to two pressure transducers (high pressure transducer and low pressure transducer). All valves are controlled by a software on the connected computer. Pressure and temperature are precisely recorded. Prior to the experiment, helium expansion is used to measure the void volume, which is defined as the total volume of helium that can penetrate in the sample cell with the sample inside. After that, the system completely evacuated and methane dosed into the reference cell. As soon as the pressure equilibrium criteria are met (pressure variation less than 0.01 bar in one minute or waiting for 30 minutes after dosing the gas into the reference cell), methane is injected into the sample cell. Methane volume dosed in the system could be calculated based on pressure, temperature, sample cell volume and the gas compressibility factor. The gas compressibility factor is determined by Peng-Robinson equation of state. The amount of adsorbed methane in sample cell is calculated by the static volumetric method as follows:

$$n_{ads} = n_{dosed} - n_{void} \tag{1}$$

Where  $n_{ads}$  is the amount of moles adsorbed by the sample,  $n_{dosed}$  is the amount of moles dosed into the system, and  $n_{void}$  is the amount of moles occupying the void volume.

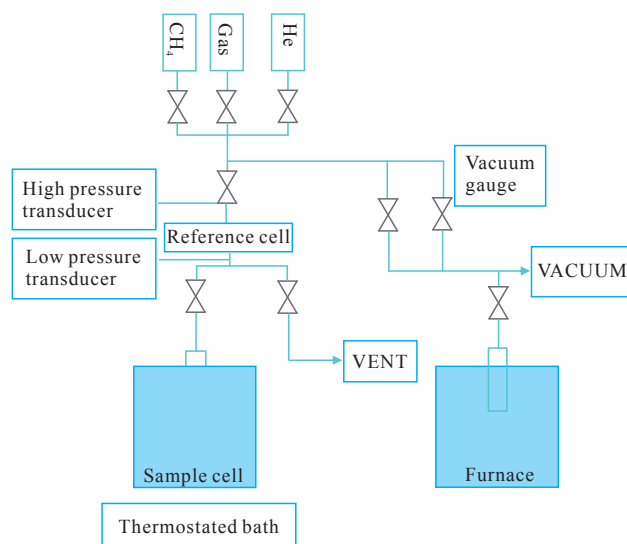


Fig. 1 Schematic diagram of high pressure volumetric analyzer

Gas adsorption is usually described by isotherms, the amount of adsorbed gas as a function of pressure at constant temperature. For methane adsorption on coal and shale, Langmuir equation is used to fit experiment result in many studies. According to Langmuir equation, the amount of adsorbed methane ( $V_{ads}$ ) can be expressed as follows:

$$V_{ads} = \frac{P}{P + P_L} \tag{2}$$

Where  $V_L$  is the Langmuir volume, defined as the maximum amount of gas that can be adsorbed on coal or shale at infinite pressure,  $P_L$  is the Langmuir pressure, defined as the pressure at which one half of the Langmuir volume can be adsorbed,  $P$  is reservoir pressure. Herein, Langmuir volume and Langmuir pressure can be determined by the following rearranged Langmuir equation:

$$\frac{P}{V_{ads}} = \frac{P}{V_L} + \frac{P_L}{V_L} \tag{3}$$

Given that experimental pressure is precisely recorded and the amount of adsorbed methane is measured, a plot of  $\frac{P}{V_{ads}}$  versus  $P$  is provided as fitted line. The slope is  $\frac{1}{V_L}$ , and the intercept is  $\frac{P_L}{V_L}$ .

### 2.2.2 Low-pressure N<sub>2</sub> sorption

Low-pressure N<sub>2</sub> adsorption and desorption isotherms were measured at 77K on a Micromeritics® Tristar II 3020 apparatus. Prior

to N<sub>2</sub> adsorption, the sample was degassed for at least 5 hours at 110°C to remove moisture and volatile in sample pores. N<sub>2</sub> adsorption volume was measured over the relative equilibrium adsorption pressure ( $P/P_0$ ) range of 0.01-0.99, where  $P$  is the gas vapour pressure in the system and  $P_0$  is the saturation pressure of N<sub>2</sub>.

The experimental data was interpreted by Brunauer-Emmett-Teller (BET) method for surface area and density functional theory (DFT) for pore size distribution. The surface area is calculated by BET method in the  $P/P_0$  range of 0.1-0.3 (Brunauer et al., 1938). Density function theory, comparing to other methods such as BJH model and DH model, can provide a description of micropores and smaller mesopores (Do and Do, 2003). Pore model is considered in density functional theory and determined by hysteresis loops. Five types of hysteresis loops have been identified by De Boer (De Boer, 1958) (Fig. 2). Type A hysteresis is correlated with cylindrical pores; type B is attributed to slit pores; type C and type D are associated with wedge shaped pores and type E is produced by bottle neck pores.

Besides, the total pore volume is obtained at maximum relative pressure ( $P/P_0=1$ ) by the assumption that pores are filled with liquid adsorbate.

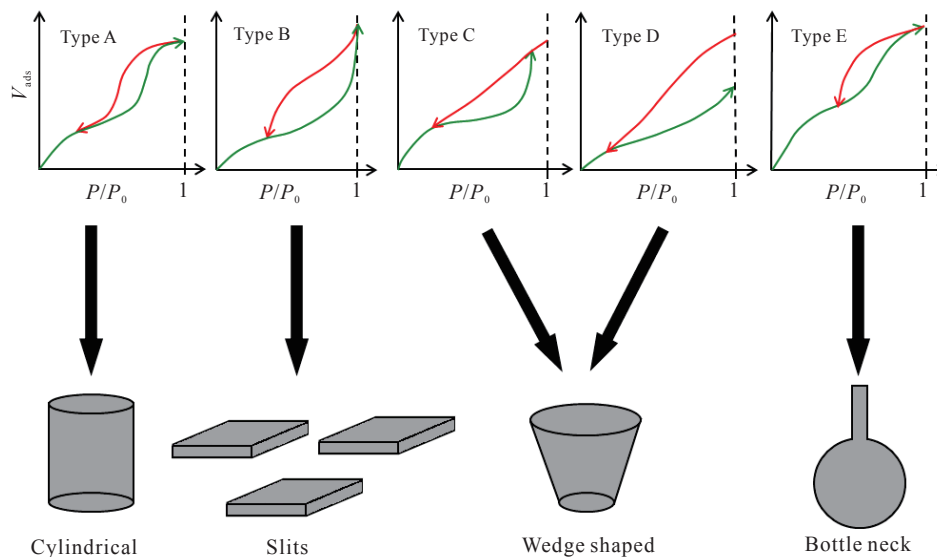


Fig. 2 Five types of hysteresis loops and corresponding pore shapes (De Boer, 1958)

## 3 Results

### 3.1 Low-pressure N<sub>2</sub> analysis

Fig. 3 shows the comparison of low-pressure N<sub>2</sub> adsorption and desorption isotherms of samples with different particle sizes. The shapes of isotherm curves reveal type II isotherm (Brunauer et al., 1940). The nitrogen adsorption at low relative pressure could be interpreted as the filling of micropores, and isotherms

rise rapidly at  $P/P_0=1$  due to the presence of macropores in the samples. As a general rule of gas adsorption, N<sub>2</sub> adsorption of all samples increases with increasing relative pressure. But the N<sub>2</sub> adsorption rate of increase is greater for the samples with smaller particle size when compared with samples with larger particle size.

As shown in Table 3, total pore volume and BET surface area increase significantly with particle size reduction. The total

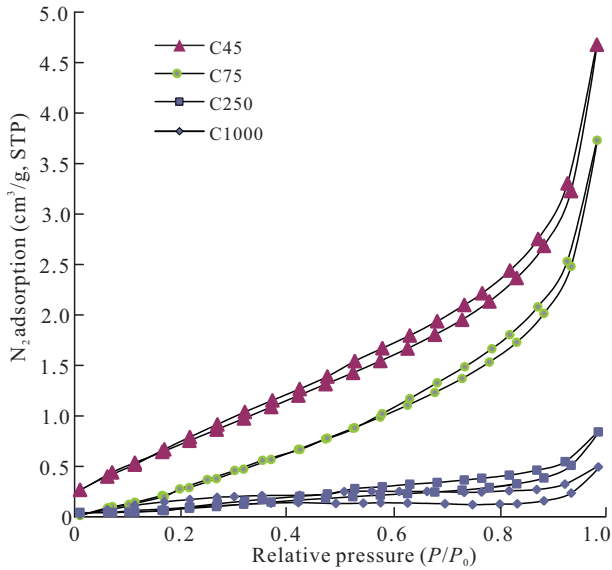


Fig. 3 Low pressure N<sub>2</sub> sorption isotherms of the studied samples at 77K: C45, C75, C250 and C1000 are sample names with particle size range in Table 3.

Table 3 Low pressure N<sub>2</sub> sorption result of the studied samples

Sample	Particle size range	BET surface area(m <sup>2</sup> /gr)	Total pore volume(cm <sup>3</sup> /100gr)	External surface area(m <sup>2</sup> /gr)	Internal surface area(m <sup>2</sup> /gr)
C45	<45μm (325mesh)	3.36	0.70	5.82E-02	3.302
C75	45~75μm (325-200mesh)	3.29	0.56	3.64E-02	3.250
C250	150~250μm (100-60mesh)	0.58	0.13	1.09E-02	0.570
C1000	850~1000μm (20-18mesh)	0.48	0.07	2.36E-03	0.480

reduction mainly results from an increase in internal surface.

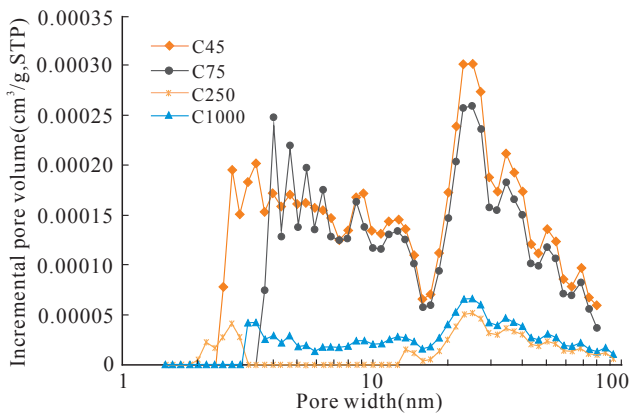


Fig. 4 Pore size distribution defined by incremental pore volume at the pore width range of 1-100nm.

Comparing with Fig. 2, hysteresis loops of the studied samples show type B. Type B hysteresis loop is produced by slit shaped pore. So slit-pore model is used in calculating pore size distribution by density function theory. Fig. 4 shows pore

pore volume of C45 sample is 0.733cm<sup>3</sup> per 100gram, which is nearly 10 times of total pore volume of C1000 sample (0.07cm<sup>3</sup> per 100gram). The BET surface area increases from 0.4757m<sup>2</sup>/g to 3.3571m<sup>2</sup>/g from the coarsest to the finest sample. The BET surface area is the summary of the internal surface area and the external surface area. It is assumed that all particles are spherical. Based on the average radius of the studied samples, external surface area can be calculated by the following formula:

$$a=6/\rho d \tag{4}$$

where  $a$  is the external surface area (with the assumption that the surface is completely smooth),  $\rho$  is the sample density,  $d$  is the particle diameter.

Given that the sample density here is the true density of coal, a value of 1.37g/cm<sup>3</sup> is used for theoretical calculation (Stanton, 1982). The external surface area of samples with different particle size is shown in Table 3. The internal surface area is obtained by subtracting external surface area from BET surface area. The increase in BET surface area with particle size

size distribution of samples with different particle size using incremental pore volume. All studied samples reveal multimodal pore size distribution and pore volume increases with decreasing particle size. Although pore size distribution among varying particle size follows the same trend for pores larger than 10nm, it is different for pores less than 10nm: the main mode of C45 is between 2.5nm to 3.7nm; the main mode of C75 is between 3.7nm to 5.0nm; the main mode of C250 is between 3.0nm to 3.7nm. Table 4 is the pore volume proportion of samples with different particle size. It is shown that the pore volume proportion of small pores (<10nm) increases with particle size reduction.

Table 4 Pore volume proportion of samples with different particle size

Sample name	Pore volume proportion of small pores(<10nm)	Pore volume proportion of big pores(>10nm)
C45	40.60%	59.40%
C75	35.70%	64.30%
C250	28.00%	72.00%
C1000	19.10%	80.90%

### 3.2 High pressure methane analysis

Fig. 5 compares methane adsorption on coal samples with different particle size. Isotherms curves for samples with different particle size are different from each other. In general, methane adsorption capacity increases with decreasing particle size at 145psi and the adsorption increase rate of the fine sample decreases rapidly with increasing pressure. C45 has the highest methane adsorption capacity at 145psi and reaches its methane adsorption peak at 870psi. C250 has low methane adsorption capacity at 145psi, but the adsorption increase rate remains stable with increasing pressure. Therefore, the methane adsorption capacity of samples at 870psi with different particle size follows this order: C75>C250>C45 >C1000.

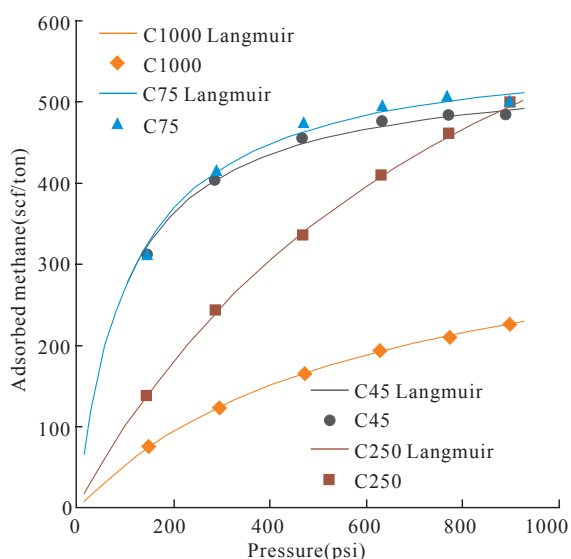


Fig. 5 Comparison of methane adsorption of samples with different particle size at 30°C. Points are the experimental results and lines are the Langmuir fitting results.

As shown in Fig. 5, methane adsorption isotherms can be well fitted by the Langmuir equation. Table 5 shows the Langmuir volume ( $V_L$ ), Langmuir pressure ( $P_L$ ) and coefficient of determination ( $R^2$ ). Among samples with varying particle size, C250 has the highest Langmuir volume.

Table 5 Langmuir parameters of samples with different particle size

Sample	$V_L$ (scf/ton)	$P_L$ (psi)	$R^2$
C45	545	101	0.999
C75	573	111	0.998
C250	984	890	0.999
C1000	378	604	0.999

## 4 Discussion

### 4.1 Effect of particle size on $N_2$ sorption

Particle size can influence pore structure of sample significantly.

The crushing sample creates new sections in particle and the sections can connect more pores to the particle surface. The introduced connectivity of pores enlarges the internal surface area and pore volume and changes pore size distribution. For coarse samples, small pores (<10nm) are neglected in that the pressure equilibrium of  $N_2$  sorption takes too much time to reach or small pores (<10nm) are isolated. As for fine sample, small pores (<10nm) are connected by new sections and pressure equilibrium of  $N_2$  sorption is easy to reach. Therefore, pore size distribution of small pores (<10nm) is different with decreasing particle size.

The hypothetical types of pores are shown in Fig. 6 (Rouquerol et al., 2014). Decreasing particle size can influence isolated pores rather than open pores (if pore channels are wide enough for probe gas). The introduced connectivity of isolated pores results in an increase in pore volume and surface area and the difference in pore size distribution. So increase in total pore volume from C1000 to C45 indicates that isolated pores for the studied coal sample is at least 10 times of open pores in terms of pore volume. Meanwhile, pore volume proportion of small pores (<10nm) increases with particle size reduction, so crushing sample connects more small pores than big pores (> 10nm). Therefore, isolated pores have more small pores (<10nm) than big pores (>10nm) in terms of pore volume.

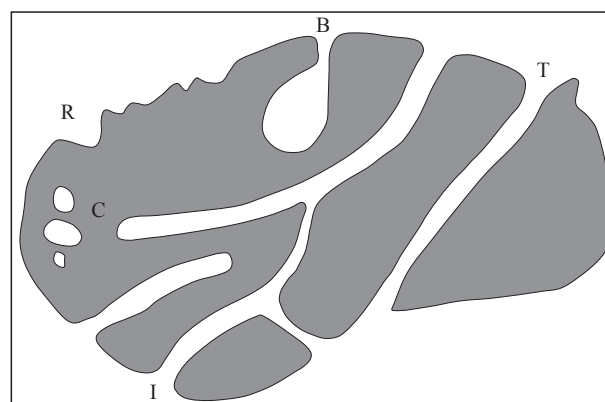


Fig. 6 Cross section of a hypothetical particle (Rouquerol et al., 2014)

### 4.2 Effect of particle size on methane sorption

Methane adsorption is closely related to particle size due to the effect of particle size on surface area, pore volume, and pore size distribution. The fine sample has enlarged surface area which provides more sites for adsorption. The sites determine methane adsorption capacity at low pressure. With increasing pressure, methane adsorption capacity increases as the general rule of gas adsorption. But if the pressure continues increasing, adsorption layers would increase and the sites would be filled up since the fine sample is mainly composed of small pores. So fine sample has low methane adsorption increase rate at high

pressure, which leads to relatively low Langmuir volume. On the other hand, coarse sample has so small surface area that methane sorption capacity is low at low pressure. However, adsorption increase rate would not decrease greatly with increasing pressure because big pores have more adsorption sites than small pores. Therefore, Langmuir volume of coarse sample is similar to fine sample but Langmuir pressure is high.

Based on the experimental results, an appropriate particle size can be recommended for high-pressure methane adsorption experiment in this study. If sample powder is too fine, much new connectivity for small pores is introduced by crushing sample. Isotherm of the fine sample would be mainly controlled by small pores. If the sample is too coarse, the time to reach pressure equilibrium would be very long. Adsorption of small pores is hard to measure, and isotherm of the coarse sample would be mainly controlled by big pores. Both small and big pores can be measured in the 150-250 $\mu\text{m}$  sample, and 150-250 $\mu\text{m}$  sample has the highest Langmuir volume. Therefore, 150-250 $\mu\text{m}$  can be used in high-pressure methane adsorption for coal.

## 5 Conclusions

Coal samples with different particle size have been measured on low-pressure  $\text{N}_2$  sorption and high-pressure methane adsorption to study if and how particle size influence high-pressure methane adsorption. The following conclusions were made.

Particle size can influence pore structure of coal sample. The crushing sample can connect closed pores to the particle surface. Isolated pores have much more pore volume than open pores in coal sample. So surface area and pore volume increase significantly with particle size reduction. Furthermore, closed pores are mainly composed of pores less than 10nm. Pore size distribution changes and proportion of pore volume increases for pores less than 10nm with particle size reduction.

Particle size has a great impact on methane adsorption since pore structure changes with particle size reduction. The fine sample has introduced much connectivity for closed pores less than 10nm, which results in that methane adsorption is mainly controlled by pores less than 10nm. Coarse sample takes too long to reach pressure equilibrium in adsorption experiment. Small pores could be neglected and methane adsorption is mainly controlled by pores larger than 10nm. 150-250 $\mu\text{m}$  is the recommended as the optimized particle size in this study as a medium sample.

## Acknowledgement

This work was conducted with support from Petroleum Engineering Department and Chemical Engineering Department

at Curtin University. We also thank our lab technician Bob Webb for his equipment support and Dr. Hongcai Wang for his helpful discussion.

## References

- Brunauer S, Deming L S, Deming W E, et al. On a theory of the van der Waals adsorption of gases. *Journal of the American Chemical Society*, 1940, 62: 1723-1732.
- Brunauer S, Emmett P H, Teller E. Adsorption of gases in multimolecular layers. *Journal of the American Chemical Society*, 1938, 60: 309-319.
- Chalmers G R L and Bustin R M. The organic matter distribution and methane capacity of the Lower Cretaceous strata of Northeastern British Columbia, Canada. *International Journal of Coal Geology*, 2007a, 70: 223-239.
- Chalmers G R L and Bustin R M. On the effects of petrographic composition on coalbed methane sorption. *International Journal of Coal Geology*, 2007b, 69: 288-304.
- Chen Y, Wei L, Mastalerz M, et al. The effect of analytical particle size on gas adsorption porosimetry of shale. *International Journal of Coal Geology*, 2015, 138: 103-112.
- Clarkson C R and Bustin R M. The effect of pore structure and gas pressure upon the transport properties of coal: A laboratory and modeling study. 1. Isotherms and pore volume distributions. *Fuel*, 1999, 78: 1333-1344.
- De Boer J. The shape of capillaries: The structure and properties of porous materials. London: Butterworths Scientific Publications, 1958, 68-92.
- Do D D and Do H D. Pore characterization of carbonaceous materials by DFT and GCMC simulations: A review. *Adsorption Science & Technology*, 2003, 21: 389-423.
- Gasparik M, Bertier P, Gensterblum Y, et al. Geological controls on the methane storage capacity in organic-rich shales. *International Journal of Coal Geology*, 2014, 123: 34-51.
- Ji L, Zhang T, Milliken K L, et al. Experimental investigation of main controls to methane adsorption in clay-rich rocks. *Applied Geochemistry*, 2012, 27: 2533-2545.
- Labani M M, Rezaee R, Saeedi A, et al. Evaluation of pore size spectrum of gas shale reservoirs using low pressure nitrogen adsorption, gas expansion and mercury porosimetry: A case study from the Perth and Canning Basins, Western Australia. *Journal of Petroleum Science and Engineering*, 2013, 112: 7-16.
- Lutynski M and González M G. Characteristics of carbon dioxide sorption in coal and gas shale – The effect of particle size. *Journal of Natural Gas Science and Engineering*, 2016, 28: 558-565.
- Ross D J K. and Bustin R M. The importance of shale composition and pore structure upon gas storage potential of shale gas reservoirs. *Marine and Petroleum Geology*, 2009, 26: 916-927.
- Rouquerol F, Rouquerol J, Llewellyn P, et al. Introduction, adsorption by powders and porous solids (Second Edition). Oxford: Academic Press, 2014, 1-24.
- Stanton R. W. Determination of the true density of pulverized coal samples. Open-File Report, 1982.
- Zhang T, Ellis G S, Ruppel S C, et al. Effect of organic-matter type and thermal maturity on methane adsorption in shale-gas systems. *Organic Geochemistry*, 2012, 47: 120-131.